Fundamentals of 3D Two-Hop Cellular Networks Analysis with Wireless Backhauled UAVs

Morteza Banagar and Harpreet S. Dhillon

***Abstract*—This paper provides the performance characterization of a three-dimensional (3D) two-hop decode-and-forward (DF) aerial-terrestrial communication network, where unmanned aerial vehicles (UAVs) coexist with terrestrial base stations (BSs) to serve a set of user equipment (UE) on the ground. We assume that each UE connects either to a BS via access link or through a UAV to a BS via joint access and backhaul links, where the link from the UE to the UAV is an access link and from the UAV to the BS is a backhaul link. To capture the impact of directionality in practical antennas, we use a model developed by the third generation partnership project (3GPP) for the antenna radiation pattern of both BSs and UAVs. Following the nearest neighbor association policy, we obtain the joint distance and angle distribution of the serving UAV to the origin in a 3D setting using tools from stochastic geometry. Furthermore, we identify and analyze key mathematical constructs as the building blocks of characterizing the received signal-to-interference-plus-noise ratio (SINR) distribution at the typical UE for the DF relaying protocol. Using these intermediate results, we derive an exact mathematical expression for the coverage probability in UAV-assisted two-hop DF cellular networks. One key takeaway from our analysis is the existence of a *mean* UAV height and a 3D density of UAVs that optimize the network coverage performance.**

***Index Terms*—UAV, 3D network, wireless backhaul, stochastic geometry, decode-and-forward, aerial-terrestrial coexistence.**

I. Introduction

Recently, there has been a lot of interest in using UAVs as wireless transceivers due to their easy and cost-effective deployment, agility, and high probability of line-of-sight [2]. UAVs can act as aerial UEs, cellular BSs, or wireless relays with a multitude of applications, such as package delivery, providing temporary service in case of large gatherings or natural disasters, and coverage extension. Although terrestrial BSs are mostly connected to the core network via strong fiber links, UAVs need to be wirelessly backhauled to the BSs first, as they usually do not have "wired" connections to the ground. Given the fact that BS antenna arrays are normally tilted downward to serve the UEs on the ground, UAVs will be served by BS antenna sidelobes, and thus, providing a reliable wireless backhaul link to the UAVs becomes very challenging. Inspired by this observation, we present a comprehensive performance analysis of 3D aerial-terrestrial cellular networks, in which BSs provide wireless backhaul to the UAVs.

Related Works. Stochastic geometry has been used extensively in the past decade to study a variety of wireless networks [3]–[5]. In particular, due to the emergence of UAVs as potential wireless transceivers with random placements and movements, there has been a surge of interest in using stochastic geometry for the system-level analysis of these aerial networks [6]–[12]. Assuming a binomial point process (BPP) to model the locations of a finite network of UAVs [6], the coexistence of UAVs with an infinite network of BSs distributed as a Poisson point process (PPP) is considered in [7], where the authors derived the overall coverage probability and area spectral efficiency of the network using a probabilistic channel model. Similarly in [8] and [9], the received rate at the typical terrestrial and aerial UE, respectively, is derived in a vertical heterogeneous network. Performance analysis of mobile UAV networks is studied in [10]–[12], where the authors considered various canonical mobility models, such as straight-line and random waypoint, for the analysis of average rate and handover probability. The authors in [13] provided a system-level analysis of two-hop DF terrestrial networks using stochastic geometry and optimization theory. As the number of terrestrial and aerial BSs/transceivers grows rapidly, it is quite natural that some of them are wirelessly backhauled to the core network [14]. Using tools from stochastic geometry, the authors in [15] studied the impact of UAV millimeter-wave (mmWave) backhauling in an aerial-terrestrial network. As mmWave networks suffer from severe link blockages, the authors in [16] considered the use of UAV-relays in a flexible backhaul architecture for dynamically rerouting to alternative paths to avoid blockages. The problem of finding the success probability of establishing a UAV wireless backhaul network using directional antenna arrays is analyzed in [17]. Despite these existing works, the comprehensive coverage analysis of 3D two-hop aerial-terrestrial cellular networks (where BSs provide wireless backhaul to the UAVs) is still an open problem, which is the main focus of this paper.

Contributions and Outcomes. Using practical antenna models proposed by the 3GPP studies [18], this paper characterizes the performance analysis of 3D backhaul-aware two-hop cellular networks, where UAVs and BSs coexist to serve the ground UEs. In particular, fiber-backhauled BSs are modeled as a 2D homogeneous PPP at a constant height above the ground, while UAVs are modeled as a 3D homogeneous PPP hovering between two permissible heights and are wirelessly backhauled to the BSs. Using the nearest neighbor association policy and the DF relaying protocol, we adopt a hybrid scheme [19] in which UEs connect either directly to the serving BS (access-only), or indirectly via the serving UAV to the serving BS (joint access and backhaul), whichever provides higher received SINR. We extensively analyze this setup by first identifying the building blocks of the received SINR in the

The authors are with Wireless@VT, Department of ECE, Virginia Tech, Blacksburg, VA. Email: {mbanagar, hdhillon}@vt.edu. The support of the US NSF (Grants CNS-1923807 and AST-2037870) is gratefully acknowledged. The extended journal version of this paper can be found on arXiv [1].

DF relaying protocol. Using tools from stochastic geometry in our 3D setup, we derive the joint distance and zenith angle distribution of the serving UAV to the typical UE. Following these results, we finally provide the exact coverage probability in UAV-assisted two-hop DF cellular networks. To the best of our understanding, this is the first work that gives a comprehensive 3D backhaul-aware analysis of UAV-assisted DF cellular networks using practical antenna models.

II. System Model

We consider a network of BSs at height h_{B} that coexists with a 3D network of UAVs to serve the ground UEs. We model the projections of the BS locations onto the ground as a 2D PPP Φ_{B} with constant density λ_{B}, while the UAV locations follow a 3D PPP Φ_{D} with constant density λ_{D} in the space enclosed between heights $h_{\mathrm{D,m}}$ and $h_{\mathrm{D,M}}$, independently from Φ_{B}. The UEs are distributed on the ground as another 2D PPP Φ_{U}, where we perform our analysis for the *typical UE* located at the origin $\mathbf{o}=(0,0,0)$ of the 3D coordinate system. Using subscript '0' to indicate the serving BS and UAV, we represent the 3D and 2D (i.e., horizontal) distances from the serving BS (resp. serving UAV) located at B_0 (resp. D_0) to $\mathbf{o}$ by r_{B_0} and u_{B_0} (resp. r_{D_0} and u_{D_0}), respectively, as shown in Fig. 1. Similarly, $\mathrm{B}_{\mathbf{x}}$, $r_{\mathrm{B}_{\mathbf{x}}}$, and $u_{\mathrm{B}_{\mathbf{x}}}$ (resp. $\mathrm{D}_{\mathbf{x}}$, $r_{\mathrm{D}_{\mathbf{x}}}$, and $u_{\mathrm{D}_{\mathbf{x}}}$) are, respectively, defined as the location of any BS in Φ_{B} (resp. any UAV in Φ_{D}) and its 3D and 2D distances to $\mathbf{o}$. Furthermore, the 3D distance between B_0 and D_0 and the zenith angle of the serving UAV to $\mathbf{o}$ are denoted as $r_{\mathrm{B}_0\mathrm{D}_0}$ and θ_{D_0}, respectively.

Following realistic antenna patterns developed by 3GPP studies [18], we assume each BS is equipped with a uniform linear array (ULA) with $N_{\mathrm{B}}=8$ equally-spaced antenna elements, where each element is an omnidirectional antenna that has a normalized power pattern (in dB) of $G_{\mathrm{E}}(\theta)=G_{\mathrm{E}}^{\max}-\min\{12(\frac{\theta-\pi/2}{\theta_{3\mathrm{dB}}})^2,\mathrm{SLA}\}$, where $G_{\mathrm{E}}^{\max}=8$ dBi is the maximum gain, $\theta_{3\mathrm{dB}}=65^\circ$ is the 3dB beamwidth, and $\mathrm{SLA}=30$ dB is the sidelobe attenuation limit [18]. The array factor of the ULA can also be written as [20, Sec. 8.3.2]

$$f_{\mathrm{A}}(\theta,\theta_{\mathrm{B}})=\frac{\sin\left(N_{\mathrm{B}}\frac{\pi}{2}[\cos(\theta)-\cos(\theta_{\mathrm{B}})]\right)}{N_{\mathrm{B}}\sin\left(\frac{\pi}{2}[\cos(\theta)-\cos(\theta_{\mathrm{B}})]\right)}, \tag{1}$$

where θ and θ_{B} are the zenith angle and the downtilted direction of the BS antenna mainlobe, both measured from the z-axis, respectively. Therefore, the gain of the BS antenna array along direction θ can be written in dBi as [20, Sec. 8.4]

$$G_{\mathrm{B}}(\theta,\theta_{\mathrm{B}})=G_{\mathrm{E}}(\theta)+20\log(|f_{\mathrm{A}}(\theta,\theta_{\mathrm{B}})|). \tag{2}$$

We assume each UAV has two antennas, one for backhaul and the other for access. The UAV backhaul antenna is directional and has vertical, horizontal, and 3D radiation patterns (in dB) of $G_{\mathrm{V}}(\theta,\theta_0)=-\min\{12(\frac{\theta-\theta_0}{\theta_{3\mathrm{dB}}})^2,\mathrm{SLA}\}$, $G_{\mathrm{H}}(\phi,\phi_0)=-\min\{12(\frac{\phi-\phi_0}{\phi_{3\mathrm{dB}}})^2,A_{\mathrm{m}}\}$, and $G_{\mathrm{D}}^{\mathrm{BH}}(\theta,\phi,\theta_0,\phi_0)=G^{\max}-\min\{-G_{\mathrm{V}}(\theta,\theta_0)-G_{\mathrm{H}}(\phi,\phi_0),A_{\mathrm{m}}\}$, respectively, where (θ_0,ϕ_0) is the antenna direction, $G^{\max}=8$ dBi is the maximum gain, $\theta_{3\mathrm{dB}}=10^\circ$ and $\phi_{3\mathrm{dB}}=10^\circ$ are the vertical and horizontal 3dB beamwidths, $\mathrm{SLA}=30$ dB, $A_{\mathrm{m}}=30$ dB is the front-back ratio [18], and the superscript BH stands for "backhaul". The UAV access antenna is omnidirectional and tilted completely toward the ground, and similar to the BS antenna elements, its gain can be written in dBi as

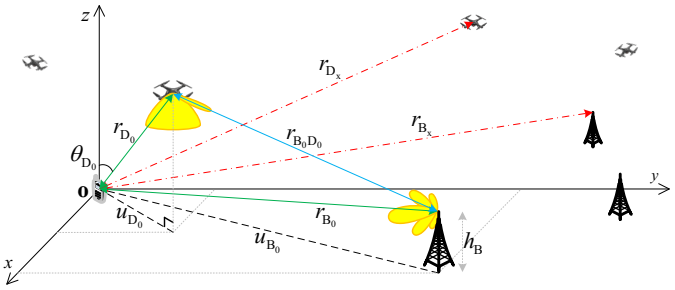

Fig. 1. An illustration of the system model. Solid green and dotted red lines denote the desired and interfering signals, respectively. Also, access and backhaul links are shown as solid green and blue lines, respectively.

$$G_{\mathrm{D}}^{\mathrm{AC}}(\theta)=G^{\max}-\min\left\{12\left(\frac{\theta-\pi}{\theta_{3\mathrm{dB}}}\right)^2,\mathrm{SLA}\right\}, \tag{3}$$

where $G^{\max}=8$ dBi, $\theta_{3\mathrm{dB}}=120^\circ$, $\mathrm{SLA}=30$ dB, and the superscript AC stands for "access". As for the UEs, we assume isotropic antennas with 0 dBi gains in all directions.

Assuming that BSs have strong fiber backhaul links to the core network and UAVs are wirelessly backhauled to the BSs, we consider two service models for connecting UEs to the core network: (i) access only, where a BS-UE link is formed, and (ii) joint access and backhaul, where BS-UAV (backhaul) and UAV-UE (access) links are formed. We assume the nearest neighbor association policy in this paper, and thus, the closest BS and UAV to the typical UE are regarded as the serving BS and UAV, respectively. The received SINR at the typical UE from the serving BS and UAV are defined, respectively, as

$$\mathrm{SINR}_{\mathrm{BU}}=\frac{P_{\mathrm{B}_0}^{\mathrm{Rx}}}{I_{\mathrm{U}}+P_{\mathrm{D}_0}^{\mathrm{Rx}}+N_0},\quad \mathrm{SINR}_{\mathrm{DU}}=\frac{P_{\mathrm{D}_0}^{\mathrm{Rx}}}{I_{\mathrm{U}}+P_{\mathrm{B}_0}^{\mathrm{Rx}}+N_0}, \tag{4}$$

where $P_{\mathrm{B}_0}^{\mathrm{Rx}}=P_{\mathrm{B}}G_{\mathrm{B}_0}f_{\mathrm{B}_0}r_{\mathrm{B}_0}^{-\alpha}$ and $P_{\mathrm{D}_0}^{\mathrm{Rx}}=P_{\mathrm{D}}G_{\mathrm{D}_0}f_{\mathrm{D}_0}r_{\mathrm{D}_0}^{-\alpha}$ are the received powers at the typical UE from the serving BS and UAV, respectively, N_0 is the noise power, and $I_{\mathrm{U}}=I_{\mathrm{BU}}+I_{\mathrm{DU}}$ is the total interference from the BSs (I_{BU}) and UAVs (I_{DU}) at the typical UE, where $I_{\mathrm{BU}}=\sum_{\mathrm{B}_{\mathbf{x}}\in\Phi_{\mathrm{B}}'}P_{\mathrm{B}}G_{\mathrm{B}_{\mathbf{x}}}f_{\mathrm{B}_{\mathbf{x}}}r_{\mathrm{B}_{\mathbf{x}}}^{-\alpha}$ and $I_{\mathrm{DU}}=\sum_{\mathrm{D}_{\mathbf{x}}\in\Phi_{\mathrm{D}}'}P_{\mathrm{D}}G_{\mathrm{D}_{\mathbf{x}}}f_{\mathrm{D}_{\mathbf{x}}}r_{\mathrm{D}_{\mathbf{x}}}^{-\alpha}$. Furthermore, assuming that the total interference at the serving UAV is negligible due to the directionality of antennas, we write the received SINR at the serving UAV from the serving BS as $\mathrm{SINR}_{\mathrm{BD}}=\frac{P_{\mathrm{B}_0\mathrm{D}_0}^{\mathrm{Rx}}}{N_0}$, where $P_{\mathrm{B}_0\mathrm{D}_0}^{\mathrm{Rx}}=P_{\mathrm{B}}g_{\mathrm{B}_0}g_{\mathrm{D}_0}f_{\mathrm{B}_0\mathrm{D}_0}r_{\mathrm{B}_0\mathrm{D}_0}^{-\alpha}$ is the received power at the serving UAV from the serving BS. We summarize the parameters in these equations as follows: α is the path-loss exponent, P_{B} and P_{D} are the transmit powers of the BSs and UAVs, G_{B_0} and G_{D_0} are the serving BS and UAV antenna gains along the direction of the typical UE, g_{B_0} and g_{D_0} are the serving BS and UAV antenna gains toward each other, f_{B_0}, f_{D_0}, and $f_{\mathrm{B}_0\mathrm{D}_0}$ are the fading powers between the serving BS and the typical UE, the serving UAV and the typical UE, and the serving BS and the serving UAV, $\Phi_{\mathrm{B}}'\equiv\Phi_{\mathrm{B}}\backslash\mathrm{B}_0$ and $\Phi_{\mathrm{D}}'\equiv\Phi_{\mathrm{D}}\backslash\mathrm{D}_0$ are the set of interfering BSs and UAVs, and the other parameters ($G_{\mathrm{B}_{\mathbf{x}}}$, $G_{\mathrm{D}_{\mathbf{x}}}$, $f_{\mathrm{B}_{\mathbf{x}}}$, $f_{\mathrm{D}_{\mathbf{x}}}$) are defined similarly.

We assume Nakagami-m fading model to capture a variety of fading environments, and thus, all channel fading powers

(i.e., f_{B_0}, f_{D_0}, $f_{\mathrm{B}_0\mathrm{D}_0}$, $f_{\mathrm{B}_\mathbf{x}}$, and $f_{\mathrm{D}_\mathbf{x}}$) are distributed as gamma random variables with cumulative distribution function (cdf) and probability density function (pdf) of $F_x(x) = \frac{1}{\Gamma(m)}\gamma(m, mx)$ and $f_X(x) = \frac{m^m}{\Gamma(m)}x^{m-1}\mathrm{e}^{-mx}$, respectively, where $\gamma(s,x) = \int_0^x t^{s-1}\mathrm{e}^{-t}\,\mathrm{d}t$ is the lower incomplete gamma function and $\Gamma(s) = \gamma(s,\infty)$ is the gamma function. We further assume that m is integer for mathematical tractability.

We adopt the DF relaying protocol, where the received signal from the source (BS) at the relay (UAV) is first decoded, then re-encoded, and finally forwarded to the destination (UE). The DF end-to-end SINR can be written as $\mathrm{SINR}_{\mathrm{e2e}} = \min\{\mathrm{SINR}_{\mathrm{BD}}, \mathrm{SINR}_{\mathrm{DU}}\}$. In this paper, we use a hybrid scheme where the UE can be served either by the BS-UE access link or by both the BS-UAV (backhaul) and UAV-UE (access) links, whichever provides higher throughput [19]. Hence, we write the received SINR at the typical UE as

$$\mathrm{SINR} = \max\{\mathrm{SINR}_{\mathrm{BU}}, \mathrm{SINR}_{\mathrm{e2e}}\}. \tag{5}$$

We now define coverage probability to evaluate the network performance as $P_{\mathrm{C}} = \mathbb{P}[\mathrm{SINR} \geq \tau]$, i.e, the probability that the received SINR at the typical UE exceeds a threshold τ.

III. Coverage Probability

In order to rigorously analyze the network coverage probability, we first study key mathematical constructs involved in the analysis of SINR of UAV-assisted two-hop networks and a specific useful property of 3D PPPs. For ease of notation, we represent the BS-UE, UAV-UE, and BS-UAV SINR values given in Section II as

$$\mathrm{SINR}_{\mathrm{BU}} = \frac{aX}{bY+I},\ \mathrm{SINR}_{\mathrm{DU}} = \frac{bY}{aX+I},\ \mathrm{SINR}_{\mathrm{BD}} = \frac{cZ}{N_0}, \tag{6}$$

where $X = f_{\mathrm{B}_0}$, $Y = f_{\mathrm{D}_0}$, $Z = f_{\mathrm{B}_0\mathrm{D}_0}$, $a = P_{\mathrm{B}}G_{\mathrm{B}_0}r_{\mathrm{B}_0}^{-\alpha}$, $b = P_{\mathrm{D}}G_{\mathrm{D}_0}r_{\mathrm{D}_0}^{-\alpha}$, $c = P_{\mathrm{B}}g_{\mathrm{B}_0}g_{\mathrm{D}_0}r_{\mathrm{B}_0\mathrm{D}_0}^{-\alpha}$, and $I = I_{\mathrm{U}} + N_0$. The following lemma provides the statistics of necessary functions for the analysis of DF two-hop networks.

Lemma 1. *Let $X \sim \Gamma(m,m)$ and $Y \sim \Gamma(m,m)$ be two independent gamma random variables, and a, b, and I be given non-negative constants. The cdf of $T_1 = \frac{aX}{bY+I}$ and $T_2 = \frac{\max\{aX,bY\}}{\min\{aX,bY\}+I}$ can be written, respectively, as*

$$F_{T_1}(\tau) = 1 - \sum_{i=0}^{m-1}\sum_{k=0}^{i}\frac{(k+m-1)!}{k!(m-1)!(i-k)!} \times \frac{a^m(b\tau)^k}{(a+b\tau)^{m+k}}\left(\frac{m\tau}{a}I\right)^{i-k}\mathrm{e}^{-\frac{m\tau}{a}I} \tag{7}$$

$$F_{T_2}(\tau) = \sum_{i=0}^{m-1}\frac{\gamma\left(m+i, \left(\frac{1}{a}+\frac{1}{b}\right)\frac{m\tau}{|1-\tau|\mathbf{1}(\tau<1)}I\right)}{i!(m-1)!}\frac{a^m b^i + a^i b^m}{(a+b)^{m+i}} - \sum_{i=0}^{m-1}\sum_{k=0}^{i}\frac{\gamma\left(m+k, \left(\frac{\tau}{a}+\frac{1}{b}\right)\frac{m\tau}{|1-\tau|\mathbf{1}(\tau<1)}I\right)}{k!(m-1)!(i-k)!} \times \frac{a^m(b\tau)^k}{(a+b\tau)^{m+k}}\left(\frac{m\tau}{a}I\right)^{i-k}\mathrm{e}^{-\frac{m\tau}{a}I} - \sum_{i=0}^{m-1}\sum_{k=0}^{i}\frac{\gamma\left(m+k, \left(\frac{1}{a}+\frac{\tau}{b}\right)\frac{m\tau}{|1-\tau|\mathbf{1}(\tau<1)}I\right)}{k!(m-1)!(i-k)!}$$

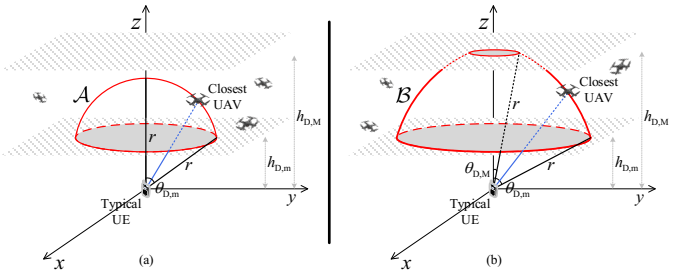

Fig. 2. The 3D network setting when the serving UAV is at distance r from $\mathbf{o}$ for (a) $h_{\mathrm{D,m}} \leq r \leq h_{\mathrm{D,M}}$, and (b) $r > h_{\mathrm{D,M}}$.

$$\times \frac{(a\tau)^k b^m}{(a\tau+b)^{k+m}}\left(\frac{m\tau}{b}I\right)^{i-k}\mathrm{e}^{-\frac{m\tau}{b}I}, \tag{8}$$

where $\mathbf{1}(.)$ is the indicator function.

Proof: See Appendix A. ∎

Remark 1. *As $\tau \to 0$ and $\tau \to \infty$, both cdfs tend to 0 and 1, respectively. For T_1 and when $\tau \to 0$, all the terms in the double summation are 0, except for $i = k = 0$, which is 1, making $F_{T_1}(0) = 0$. When $\tau \to \infty$, the double summation will be 0, making $F_{T_1}(\infty) = 1$. For T_2 and when $\tau \to 0$, since $\gamma(s,0) = 0$ for all s, we have $F_{T_2}(0) = 0$. When $\tau \to \infty$, the double summations are both 0, while the single summation is equal to 1 [21, Eq. (1.78)], and thus, $F_{T_2}(\infty) = 1$.*

Considering the point process of BSs and using the nearest neighbor association policy, we provide the serving BS distance distribution in the next lemma, which has a straightforward proof using the null probability of PPP Φ_{B} [3].

Lemma 2. *The cdf and pdf of the serving BS distance to the typical UE can be written as $F_{r_{\mathrm{B}_0}}(r) = 1 - \mathrm{e}^{-\pi\lambda_{\mathrm{B}}(r^2 - h_{\mathrm{B}}^2)}$ and $f_{r_{\mathrm{B}_0}}(r) = 2\pi\lambda_{\mathrm{B}} r\mathrm{e}^{-\pi\lambda_{\mathrm{B}}(r^2-h_{\mathrm{B}}^2)}$, respectively.*

In the course of the following two lemmas, we derive the *joint distance and angle* distribution of the serving UAV to the typical UE in our 3D aerial setting.

Lemma 3. *The cdf and pdf of the serving UAV distance to the typical UE can be written as $F_{r_{\mathrm{D}_0}}(r) = 1 - \mathrm{e}^{-\pi\lambda_{\mathrm{D}}\beta(r)}$ and*

$$f_{r_{\mathrm{D}_0}}(r) = 2\pi\lambda_{\mathrm{D}} r^2\left(\cos(\theta_{\mathrm{D,M}}(r)) - \cos(\theta_{\mathrm{D,m}}(r))\right)\mathrm{e}^{-\pi\lambda_{\mathrm{D}}\beta(r)},$$

respectively, where

$$\theta_{\mathrm{D,m}}(r) = \cos^{-1}\left(\frac{h_{\mathrm{D,m}}}{r}\right),\quad \theta_{\mathrm{D,M}}(r) = \cos^{-1}\left(\min\left\{\frac{h_{\mathrm{D,M}}}{r}, 1\right\}\right),$$
$$\beta(r) = r^3\left[\cos(\theta_{\mathrm{D,M}}(r)) - \cos(\theta_{\mathrm{D,m}}(r))\right] - \frac{1}{3}r^3\left[\cos^3(\theta_{\mathrm{D,M}}(r)) - \cos^3(\theta_{\mathrm{D,m}}(r))\right]$$

Proof: Consider the 3D setting in Fig. 2. We have

$$F_{r_{\mathrm{D}_0}}(r) = \mathbb{P}[r_{\mathrm{D}_0} \leq r] = 1 - \mathbb{P}[\text{No UAV in } \mathcal{A} \text{ or } \mathcal{B}]$$
$$= 1 - \mathrm{e}^{-\Lambda(\mathcal{A})}\mathbf{1}(h_{\mathrm{D,m}} \leq r \leq h_{\mathrm{D,M}}) - \mathrm{e}^{-\Lambda(\mathcal{B})}\mathbf{1}(r > h_{\mathrm{D,M}})$$

$$\overset{(a)}{=} 1 - \begin{cases} \exp\Big[-\int_0^{2\pi}\int_0^{\cos^{-1}(\frac{h_{\mathrm{D,m}}}{r})} \int_{\frac{h_{\mathrm{D,m}}}{\cos(\theta_1)}}^{r} \lambda_{\mathrm{D}} \\ \qquad \times r_1^2 \sin(\theta_1)\,\mathrm{d}r_1\,\mathrm{d}\theta_1\,\mathrm{d}\phi_1\Big] & r \le h_{\mathrm{D,M}} \\ \exp\Big[-\int_0^{2\pi}\int_0^{\cos^{-1}(\frac{h_{\mathrm{D,M}}}{r})} \int_{\frac{h_{\mathrm{D,m}}}{\cos(\theta_1)}}^{\frac{h_{\mathrm{D,M}}}{\cos(\theta_1)}} \lambda_{\mathrm{D}} \\ \qquad \times r_1^2 \sin(\theta_1)\,\mathrm{d}r_1\,\mathrm{d}\theta_1\,\mathrm{d}\phi_1 \\ \quad -\int_0^{2\pi}\int_{\cos^{-1}(\frac{h_{\mathrm{D,M}}}{r})}^{\cos^{-1}(\frac{h_{\mathrm{D,m}}}{r})} \int_{\frac{h_{\mathrm{D,m}}}{\cos(\theta_1)}}^{r} \lambda_{\mathrm{D}} \\ \qquad \times r_1^2 \sin(\theta_1)\,\mathrm{d}r_1\,\mathrm{d}\theta_1\,\mathrm{d}\phi_1\Big] & r > h_{\mathrm{D,M}} \end{cases},$$

where $\Lambda(\mathcal{S})$ is the intensity measure of set $\mathcal{S}$ and (r_1, θ_1, ϕ_1) is the spherical coordinate triplet. We derived the null probability of 3D PPP Φ_{D} in (a) by integrating its density over the spherical cap $\mathcal{A}$ for $h_{\mathrm{D,m}} \le r \le h_{\mathrm{D,M}}$ (Fig. 2 (a)) and the spherical segment $\mathcal{B}$ for $r > h_{\mathrm{D,M}}$ (Fig. 2 (b)). Evaluating these integrals and taking their derivatives w.r.t. r, we obtain the cdf and pdf of r_{D_0} as given in the lemma statement. ■

Lemma 4. *The joint pdf of the distance and zenith angle of the serving UAV to the typical UE can be written as*

$$f_{r_{\mathrm{D}_0},\theta_{\mathrm{D}_0}}(r,\theta) = 2\pi\lambda_{\mathrm{D}} r^2 \mathrm{e}^{-\pi\lambda_{\mathrm{D}}\beta(r)} \times \sin(\theta)\mathbf{1}(\theta_{\mathrm{D,M}}(r) \le \theta \le \theta_{\mathrm{D,m}}(r)), \quad (9)$$

where $\theta_{\mathrm{D,m}}(r)$, $\theta_{\mathrm{D,M}}(r)$, and $\beta(r)$ are as given in Lemma 3.

Proof: To obtain the joint pdf of r_{D_0} and θ_{D_0}, we first derive the conditional pdf $f_{\theta_{\mathrm{D}_0}|r_{\mathrm{D}_0}}(\theta|r)$. Conditioned on $r_{\mathrm{D}_0} = r$, the serving UAV is distributed uniformly on the surface of the spherical cap $\mathcal{A}$ or the spherical segment $\mathcal{B}$. Since the differential element of solid angle Ω for a sphere is given as $\mathrm{d}\Omega = r^2\sin(\theta)\mathrm{d}r\mathrm{d}\theta\mathrm{d}\phi = -r^2\mathrm{d}r\mathrm{d}(\cos(\theta))\mathrm{d}\phi$, we conclude that $\cos(\theta)$ should be uniformly distributed between $\cos(\theta_{\mathrm{D,M}}(r))$ and $\cos(\theta_{\mathrm{D,m}}(r))$. Hence, we have

$$f_{\theta_{\mathrm{D}_0}|r_{\mathrm{D}_0}}(\theta|r) = \frac{\sin(\theta)\mathbf{1}(\theta_{\mathrm{D,M}}(r) \le \theta \le \theta_{\mathrm{D,m}}(r))}{\cos(\theta_{\mathrm{D,M}}(r)) - \cos(\theta_{\mathrm{D,m}}(r))}.$$

Now, using the identity $f_{r_{\mathrm{D}_0},\theta_{\mathrm{D}_0}}(r,\theta) = f_{\theta_{\mathrm{D}_0}|r_{\mathrm{D}_0}}(\theta|r) f_{r_{\mathrm{D}_0}}(r)$ and the previous lemma, we obtain (9). ■

Remark 2. *The random variables r_{D_0} and θ_{D_0} are clearly dependent. However, this dependency becomes less significant as $|h_{\mathrm{D,M}} - h_{\mathrm{D,m}}| \to \infty$. In fact, when UAVs are distributed as a 3D PPP in the half-space $z \ge 0$, r_{D_0} and θ_{D_0} will become independent from each other and we have*

$$f_{r_{\mathrm{D}_0}}(r) = 2\pi\lambda_{\mathrm{D}} r^2 \mathrm{e}^{-\frac{2}{3}\pi\lambda_{\mathrm{D}} r^3}, \quad f_{\theta_{\mathrm{D}_0}}(\theta) = \sin(\theta)\mathbf{1}\Big(0 \le \theta \le \frac{\pi}{2}\Big).$$

Using the previous lemmas, we state the main result of this paper in the following theorem.

Theorem 1. *The coverage probability for the DF relaying protocol can be written as*

$$P_{\mathrm{C}} = \int_0^{2\pi}\int_{h_{\mathrm{D,m}}}^{\infty}\int_{\theta_{\mathrm{D,M}}(r)}^{\theta_{\mathrm{D,m}}(r)}\int_{h_{\mathrm{B}}}^{\infty}\int_0^{\infty} W f_Z(z) f_{r_{\mathrm{B}_0}}(r_{\mathrm{B}_0}) \times f_{r_{\mathrm{D}_0},\theta_{\mathrm{D}_0}}(r,\theta) f_{\phi_{\mathrm{B}_0\mathrm{D}_0}}(\phi)\,\mathrm{d}z\,\mathrm{d}r_{\mathrm{B}_0}\,\mathrm{d}\theta\,\mathrm{d}r\,\mathrm{d}\phi, \quad (10)$$

where $Z = f_{\mathrm{B}_0\mathrm{D}_0} \sim \Gamma(m,m)$, $f_{r_{\mathrm{B}_0}}(r)$ and $f_{r_{\mathrm{D}_0},\theta_{\mathrm{D}_0}}(r,\theta)$ are given in Lemmas 2 and 4, respectively, $\phi_{\mathrm{B}_0\mathrm{D}_0} \sim U[0,2\pi)$ is the azimuthal angle between B_0 and D_0, $a = P_{\mathrm{B}} G_{\mathrm{B}_0} r_{\mathrm{B}_0}^{-\alpha}$, $b = P_{\mathrm{D}} G_{\mathrm{D}_0} r_{\mathrm{D}_0}^{-\alpha}$, $c = P_{\mathrm{B}} g_{\mathrm{B}_0} g_{\mathrm{D}_0} r_{\mathrm{B}_0\mathrm{D}_0}^{-\alpha}$, $G_{\mathrm{D}_0} = G_{\mathrm{D}}^{\mathrm{AC}}(\pi - \theta_{\mathrm{D}_0})$, $G_{\mathrm{B}_0} = G_{\mathrm{B}}(\pi - \cos^{-1}(\frac{h_{\mathrm{B}}}{r_{\mathrm{B}_0}}), \theta_{\mathrm{B}})$, $g_{\mathrm{D}_0} = G^{\max}$, $g_{\mathrm{B}_0} = G_{\mathrm{B}}(\cos^{-1}(\frac{r_{\mathrm{D}_0}\cos(\theta_{\mathrm{D}_0}) - h_{\mathrm{B}}}{r_{\mathrm{B}_0\mathrm{D}_0}}), \theta_{\mathrm{B}})$, $r_{\mathrm{B}_0\mathrm{D}_0}^2 = r_{\mathrm{B}_0}^2 + r_{\mathrm{D}_0}^2 - 2h_{\mathrm{B}} r_{\mathrm{D}_0}\cos(\theta_{\mathrm{D}_0}) - 2\sqrt{r_{\mathrm{B}_0}^2 - h_{\mathrm{B}}^2}\, r_{\mathrm{D}_0}\sin(\theta_{\mathrm{D}_0})\cos(\phi_{\mathrm{B}_0\mathrm{D}_0})$, and $W = V_1 + (1-V_0)(V_2 + V_3\mathbf{1}(\tau < 1))$, where $V_0 = \frac{\gamma(m, \frac{N_0}{c} m\tau)}{(m-1)!}$, and V_1, V_2, V_3, and the conditional Laplace transform of interference are given at the bottom of this page.

Proof: See Appendix B. ■

Remark 3. *Ignoring noise, we have $\mathrm{SINR}_{\mathrm{BD}} \to \infty$, and thus $\mathrm{SINR}_{\mathrm{e2e}} = \mathrm{SINR}_{\mathrm{DU}}$. Therefore, the coverage probability for*

$$V_1 = \sum_{i=0}^{m-1}\sum_{k=0}^{i} \binom{k+m-1}{k} \frac{a^m (b\tau)^k}{(a+b\tau)^{m+k}} \frac{(-s_1)^{i-k}}{(i-k)!} \frac{\partial^{i-k}}{\partial s_1^{i-k}} \mathcal{L}_I(s_1|\mathrm{B}_0,\mathrm{D}_0)\Big|_{s_1=\frac{1}{a}m\tau},$$

$$V_2 = \sum_{i=0}^{m-1}\sum_{k=0}^{i} \binom{k+m-1}{k} \frac{(a\tau)^k b^m}{(a\tau+b)^{k+m}} \frac{(-s_2)^{i-k}}{(i-k)!} \frac{\partial^{i-k}}{\partial s_2^{i-k}} \mathcal{L}_I(s_2|\mathrm{B}_0,\mathrm{D}_0)\Big|_{s_2=\frac{1}{b}m\tau},$$

$$V_3 = \sum_{i=0}^{m-1}\sum_{j=0}^{i+m-1} \binom{i+m-1}{i} \frac{a^m b^i + a^i b^m}{(a+b)^{m+i}} \frac{(-s_3)^j}{(j)!} \frac{\partial^j}{\partial s_3^j} \mathcal{L}_I(s_3|\mathrm{B}_0,\mathrm{D}_0)\Big|_{s_3=\frac{a+b}{ab(1-\tau)}m\tau} - \sum_{i=0}^{m-1}\sum_{k=0}^{i}\sum_{j=0}^{k+m-1} \binom{k+m-1}{k}\binom{j+i-k}{j} \times \left(\frac{\tau}{1-\tau}\right)^j \left[\frac{a^m(b\tau)^{k-j}}{(a+b\tau)^{m+k-j}} \frac{(-s_1)^{j+i-k}}{(j+i-k)!} + \frac{(a\tau)^{k-j} b^m}{(a\tau+b)^{k-j+m}} \frac{(-s_2)^{j+i-k}}{(j+i-k)!}\right] \frac{\partial^{j+i-k}}{\partial s_3^{j+i-k}} \mathcal{L}_I(s_3|\mathrm{B}_0,\mathrm{D}_0)\Big|_{s_3=\frac{a+b}{ab(1-\tau)}m\tau},$$

$$\mathcal{L}_I(s|\mathrm{B}_0,\mathrm{D}_0) = \exp\Bigg[-sN_0 - 2\pi\lambda_{\mathrm{B}} \int_{u_{\mathrm{B}_0}}^{\infty} \left[1 - \Big(1 + \frac{sP_{\mathrm{B}}}{m} \frac{G_{\mathrm{B}}\big(\pi - \tan^{-1}(\frac{u_{\mathrm{B}_\mathbf{x}}}{h_{\mathrm{B}}}), \theta_{\mathrm{B}}\big)}{\big(u_{\mathrm{B}_\mathbf{x}}^2 + h_{\mathrm{B}}^2\big)^{\frac{\alpha}{2}}}\Big)^{-m}\right] u_{\mathrm{B}_\mathbf{x}}\mathrm{d}u_{\mathrm{B}_\mathbf{x}}$$

$$- 2\pi\lambda_{\mathrm{D}} \int_{\theta_{\mathrm{D,M}}(r_{\mathrm{D}_0})}^{\theta_{\mathrm{D,m}}(r_{\mathrm{D}_0})} \int_{r_{\mathrm{D}_0}}^{\frac{h_{\mathrm{D,M}}}{\cos(\theta_{\mathrm{D}_\mathbf{x}})}} \left[1 - \Big(1 + \frac{sP_{\mathrm{D}}}{m} \frac{G_{\mathrm{D}}^{\mathrm{AC}}(\pi - \theta_{\mathrm{D}_\mathbf{x}})}{r_{\mathrm{D}_\mathbf{x}}^{\alpha}}\Big)^{-m}\right] r_{\mathrm{D}_\mathbf{x}}^2 \sin(\theta_{\mathrm{D}_\mathbf{x}})\mathrm{d}r_{\mathrm{D}_\mathbf{x}}\mathrm{d}\theta_{\mathrm{D}_\mathbf{x}}$$

$$- 2\pi\lambda_{\mathrm{D}} \int_{\theta_{\mathrm{D,m}}(r_{\mathrm{D}_0})}^{\frac{\pi}{2}} \int_{\frac{h_{\mathrm{D,m}}}{\cos(\theta_{\mathrm{D}_\mathbf{x}})}}^{\frac{h_{\mathrm{D,M}}}{\cos(\theta_{\mathrm{D}_\mathbf{x}})}} \left[1 - \Big(1 + \frac{sP_{\mathrm{D}}}{m} \frac{G_{\mathrm{D}}^{\mathrm{AC}}(\pi - \theta_{\mathrm{D}_\mathbf{x}})}{r_{\mathrm{D}_\mathbf{x}}^{\alpha}}\Big)^{-m}\right] r_{\mathrm{D}_\mathbf{x}}^2 \sin(\theta_{\mathrm{D}_\mathbf{x}})\mathrm{d}r_{\mathrm{D}_\mathbf{x}}\mathrm{d}\theta_{\mathrm{D}_\mathbf{x}}\Bigg].$$

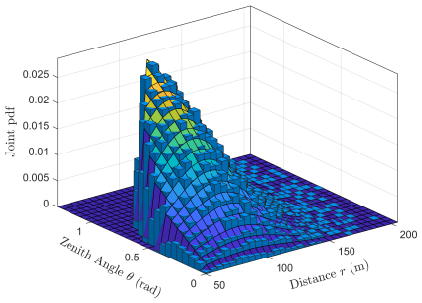

Fig. 3. The joint distribution of r_{D_0} and θ_{D_0} ($\lambda_{\mathrm{D}}=10^{-6}$, $h_{\mathrm{D,m}}=50$ m, $h_{\mathrm{D,M}}=200$ m).

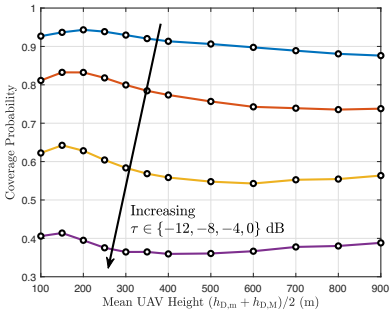

Fig. 4. Coverage probability as a function of mean UAV height ($\lambda_{\mathrm{D}}=10^{-8}$, $h_{\mathrm{D,M}}-h_{\mathrm{D,m}}=100$ m).

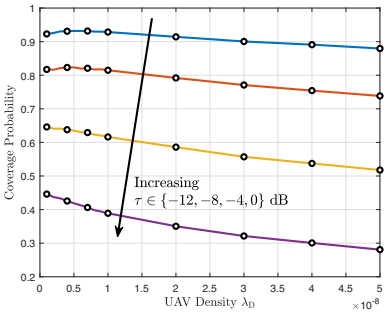

Fig. 5. Coverage probability as a function of UAV density ($h_{\mathrm{D,m}}=50$ m, $h_{\mathrm{D,M}}=200$ m).

the DF protocol in an interference-limited network is the same as given in Theorem 1 with $W = V_1+V_2+V_3\mathbf{1}(\tau<1)$, where V_1, V_2, and V_3 are given in Theorem 1 statement.

IV. Numerical Results

In this section, we verify our technical results via simulations and glean several system-level insights of our 3D setup. The simulation parameters are as follows: $\lambda_{\mathrm{B}} = 10^{-6}$ (i.e., 1 BS/km^2), $h_{\mathrm{B}} = 20$ m, λ_{D} ranges in $\{10^{-9},\ldots,10^{-6}\}$, $h_{\mathrm{D,m}}$ and $h_{\mathrm{D,M}}$ take values in $\{50,\ldots,950\}$ m, $\alpha = 3$, $m = 1$, $P_{\mathrm{B}} = 10$ dB, $P_{\mathrm{D}} = 5$ dB, $N_0 = 10^{-8}$, $N_{\mathrm{B}} = 8$, and $\theta_{\mathrm{B}} = 100^\circ$ (measured from the z-axis). In Fig. 3, we plot the joint pdf of the UAV serving distance (r_{D_0}) and zenith angle (θ_{D_0}) with $\lambda_{\mathrm{D}} = 10^{-6}$, $h_{\mathrm{D,m}} = 100$ m, and $h_{\mathrm{D,M}} = 300$ m. Note that the histogram bars are the simulation data while the surface plot is from Lemma 4. Keeping the difference between the maximum and minimum UAV heights constant (i.e., $h_{\mathrm{D,M}}-h_{\mathrm{D,m}} = 100$ m), we show the coverage probability as a function of the mean UAV height in Fig. 4. Assuming $h_{\mathrm{D,m}} = 50$ m and $h_{\mathrm{D,M}} = 200$ m, we plot the coverage probability as the UAV density is increased in Fig. 5.

As is clear from Figs. 4 and 5 and also from the definition, the coverage probability decreases as the SINR threshold τ increases. Furthermore, we observe from these figures that there is a mean UAV height h_{D}^* and UAV density λ_{D}^* for which the coverage probability is maximized for each SINR threshold τ. Increasing the average UAV height has two effects: (i) the average distance from the UAVs to the typical UE is increased, and (ii) the average zenith angle from the UAVs to the typical UE is decreased. Note that the former is detrimental to both desired and interfering signals, while the latter is favorable to both, as the UAV access antennas are omnidirectional and titled completely toward the ground (see (3)). The overall effect of these contending phenomena is an optimal mean UAV height h_{D}^* for each τ, which can be seen in Fig. 4. Similarly, increasing the average number of UAVs has three effects: (i) the mean serving UAV distance is decreased, (ii) the mean distance between the interfering UAVs and the typical UE is decreased, and (iii) the aggregate number of interferers is increased. Although the first effect is favorable, the others worsen the coverage probability, and thus, their overall impact is an optimal UAV density λ_{D}^*, as seen in Fig. 5.

V. Conclusion

In this paper, we presented the fundamentals of performance analysis of 3D two-hop DF aerial-terrestrial networks, where UAVs and BSs coexist to serve the ground UEs. A hybrid scheme is adopted, in which UEs connect either directly to BSs via access link or through UAVs to BSs via joint access and backhaul links, whichever provides higher SINR. We used realistic antenna radiation patterns developed by 3GPP for both BSs and UAVs to address the effect of directionality in practical antennas. Using tools from stochastic geometry and assuming the nearest neighbor association policy, we provided a rigorous analysis of the joint distribution of the serving UAV distance and zenith angle to the typical UE. Using this novel result and by identifying the building blocks of SINR distribution analysis, we provided an exact mathematical treatment for the coverage probability in two-hop DF cellular networks that use UAVs for wireless backhaul. To the best of our knowledge, this is the first work that offers a rigorous analysis of 3D UAV-assisted cellular networks, in which BSs provide wireless backhaul to the UAVs using a two-hop DF protocol. Extending the results of this paper to more elaborate multi-hop settings and other relaying schemes, such as amplify-and-forward, are promising future research directions.

Appendix

A. Proof of Lemma 1

By definition, we have $F_{T_1}(\tau) = \mathbb{P}\left[aX \le \tau bY + \tau I\right]$

$$= \int_0^\infty \int_0^{\frac{\tau by+\tau I}{a}} f_{X,Y}(x,y)\,\mathrm{d}x\,\mathrm{d}y \overset{(a)}{=} \int_0^\infty f_Y(y) F_X\left(\frac{\tau by+\tau I}{a}\right)\mathrm{d}y$$

$$\overset{(b)}{=} 1 - \sum_{i=0}^{m-1}\sum_{k=0}^{i} \frac{m^m(k+m-1)!}{i!(m-1)!}\binom{i}{k}\left(\frac{m\tau b}{a}\right)^i\left(\frac{I}{b}\right)^{i-k} \times \left(m+\frac{m\tau b}{a}\right)^{-m-k} \mathrm{e}^{-\frac{m\tau I}{a}},$$

where in (a) we used the independence of X and Y and in (b) we used the series expansion $F_X(x) = 1-\sum_{i=0}^{m-1}\frac{(mx)^i}{i!}\mathrm{e}^{-mx}$ for integer m and the binomial expansion to simplify the resulting integral. The final result in (7) is obtained by further mathematical manipulations. As for the cdf of T_2, we can write

$$F_{T_2}(\tau) = \mathbb{P}\left[\frac{aX}{bY+I} \le \tau, aX \ge bY\right] + \mathbb{P}\left[\frac{bY}{aX+I} \le \tau, aX < bY\right]$$

$$= \begin{cases} \int_0^{\frac{\tau I}{(1-\tau)b}} \int_{\frac{by}{a}}^{\frac{\tau by+\tau I}{a}} f_{X,Y}(x,y)\,\mathrm{d}x\,\mathrm{d}y \\ + \int_0^{\frac{\tau I}{(1-\tau)a}} \int_{\frac{ax}{b}}^{\frac{\tau ax+\tau I}{b}} f_{X,Y}(x,y)\,\mathrm{d}y\,\mathrm{d}x & \tau < 1 \\ \int_0^\infty \int_{\frac{by}{a}}^{\frac{\tau by+\tau I}{a}} f_{X,Y}(x,y)\,\mathrm{d}x\,\mathrm{d}y \\ + \int_0^\infty \int_{\frac{ax}{b}}^{\frac{\tau ax+\tau I}{b}} f_{X,Y}(x,y)\,\mathrm{d}y\,\mathrm{d}x & \tau \ge 1 \end{cases}.$$

Denote the first and second double integrals in region $\tau < 1$ as L_1 and L_2, respectively. Note that once L_1 is derived, L_2 is readily obtained by switching a and b. We have

$$L_1 \overset{(a)}{=} \int_0^{\frac{\tau I}{(1-\tau)b}} \frac{m^m}{(m-1)!} y^{m-1} \mathrm{e}^{-my} \sum_{i=0}^{m-1} \frac{1}{i!} \times \left[\left(\frac{mb}{a} y\right)^i \mathrm{e}^{-\frac{mb}{a}y} - \left(\frac{m\tau b}{a} y + \frac{m\tau}{a} I\right)^i \mathrm{e}^{-\frac{m\tau b}{a}y - \frac{m\tau}{a}I} \right] \mathrm{d}y$$

$$\overset{(b)}{=} \sum_{i=0}^{m-1} \frac{\gamma\left(m+i, \left(\frac{1}{a}+\frac{1}{b}\right)\frac{m\tau}{(1-\tau)} I\right)}{i!(m-1)!} \frac{a^m b^i}{(a+b)^{m+i}} - \sum_{i=0}^{m-1} \sum_{k=0}^{i} \frac{\gamma\left(m+k, \left(\frac{\tau}{a}+\frac{1}{b}\right)\frac{m\tau}{(1-\tau)} I\right)}{k!(m-1)!(i-k)!} \frac{a^m (b\tau)^k}{(a+b\tau)^{m+k}} \left(\frac{m\tau}{a} I\right)^{i-k} \mathrm{e}^{-\frac{m\tau}{a}I}$$

where in (a) we used the independence of X and Y and the series expansion of the cdf of gamma random variables and in (b) we first switched the order of summation and integration and then simplified the integrals using the binomial expansion and the definition of the lower incomplete gamma function. As for region $\tau \geq 1$, the proof follows the same steps as above, but becomes simpler since we end up with gamma functions instead of incomplete gamma functions. Noting that $\gamma(s, \infty) = \Gamma(s)$, we obtain the final result as given in (8). ■

B. Proof of Theorem 1

Using the definition, we can write $P_{\mathrm{C}} \triangleq \mathbb{P}\left[\mathrm{SINR} \geq \tau\right]$

$$= 1 - \mathbb{P}[\mathrm{SINR}_{\mathrm{BU}} < \tau, \min\{\mathrm{SINR}_{\mathrm{BD}}, \mathrm{SINR}_{\mathrm{DU}}\} < \tau]$$

$$= 1 + \mathbb{P}[\mathrm{SINR}_{\mathrm{BU}} < \tau, \mathrm{SINR}_{\mathrm{BD}} \geq \tau, \mathrm{SINR}_{\mathrm{DU}} \geq \tau] - \mathbb{P}[\mathrm{SINR}_{\mathrm{BU}} < \tau]$$

$$\overset{(a)}{=} 1 + \mathbb{E}\big[\mathbb{P}\left[\mathrm{SINR}_{\mathrm{BU}} < \tau, \mathrm{SINR}_{\mathrm{DU}} \geq \tau | \mathrm{B}_0, \mathrm{D}_0, I\right] \times \mathbb{P}\left[\mathrm{SINR}_{\mathrm{BD}} \geq \tau | \mathrm{B}_0, \mathrm{D}_0\right]\big] - \mathbb{E}\big[\mathbb{P}\left[\mathrm{SINR}_{\mathrm{BU}} < \tau | \mathrm{B}_0, \mathrm{D}_0, I\right]\big]$$

$$\overset{(b)}{=} 1 - \mathbb{E}\left[\mathbb{P}\left[\tfrac{aX}{bY+I} < \tau \Big| \mathrm{B}_0, \mathrm{D}_0, I\right] \mathbb{P}\left[\tfrac{cZ}{N_0} < \tau \Big| \mathrm{B}_0, \mathrm{D}_0\right]\right] - \mathbb{E}\left[\mathbb{P}\left[\tfrac{\max\{aX, bY\}}{\min\{aX, bY\}+I} < \tau \Big| \mathrm{B}_0, \mathrm{D}_0, I\right] \mathbb{P}\left[\tfrac{cZ}{N_0} \geq \tau \Big| \mathrm{B}_0, \mathrm{D}_0\right]\right], \quad (11)$$

where in (a) we conditioned the probabilities on knowing B_0, D_0, and $I = I_{\mathrm{U}} + N_0$, and in (b) we wrote the SINR terms in their simpler forms as in (6) and used the relation $\mathbb{P}\left[E \cap F\right] + \mathbb{P}\left[E \cap \bar{F}\right] = \mathbb{P}\left[E\right]$, where $E = \mathrm{SINR}_{\mathrm{BU}}$ and $F = \mathrm{SINR}_{\mathrm{DU}}$, to further simplify the result. To take these expectations w.r.t. I after using Lemma 1, we need to derive the Laplace transform of I, which can be formulated as $\mathcal{L}_I(s|\mathrm{B}_0, \mathrm{D}_0) = \mathbb{E}\big[\mathrm{e}^{-s(I_{\mathrm{U}}+N_0)}\big|\mathrm{B}_0, \mathrm{D}_0\big] = \mathrm{e}^{-sN_0}\mathbb{E}\big[\mathrm{e}^{-sI_{\mathrm{BU}}}\big|\mathrm{B}_0\big]\mathbb{E}\big[\mathrm{e}^{-sI_{\mathrm{DU}}}\big|\mathrm{D}_0\big]$ due to the independence of I_{BU} and I_{DU}. Starting with the conditional Laplace transform of I_{BU}, we have $\mathcal{L}_{I_{\mathrm{BU}}}(s|\mathrm{B}_0)$

$$= \mathbb{E}\left[\mathrm{e}^{-s\sum_{\mathrm{B_x}\in\Phi_{\mathrm{B}}'} P_{\mathrm{B}} G_{\mathrm{B_x}} r_{\mathrm{B_x}}^{-\alpha} f_{\mathrm{B_x}}} \Big| \mathrm{B}_0\right] \overset{(a)}{=} \mathbb{E}\left[\prod_{\mathrm{B_x}\in\Phi_{\mathrm{B}}'} \left(1 + \tfrac{sP_{\mathrm{B}}}{m} \tfrac{G_{\mathrm{B_x}}}{r_{\mathrm{B_x}}^{\alpha}}\right)^{-m} \Big| \mathrm{B}_0\right]$$

$$\overset{(b)}{=} \exp\left[-2\pi\lambda_{\mathrm{B}} \int_{u_{\mathrm{B}_0}}^{\infty} \left[1 - \left(1 + \frac{sP_{\mathrm{B}}}{m} \frac{G_{\mathrm{B_x}}}{r_{\mathrm{B_x}}^{\alpha}}\right)^{-m}\right] u_{\mathrm{B_x}} \mathrm{d}u_{\mathrm{B_x}}\right],$$

where in (a) we took the moment generating function (mgf) of the gamma random variable $f_{\mathrm{B_x}}$, and in (b) we used the probability generating functional (pgfl) of the 2D PPP Φ_{B}'. Similarly, we can write the conditional Laplace transform of I_{DU} as above with the only difference being the 3D setting. Therefore, the integration in step (b) would be over the space enclosed between $z = h_{\mathrm{D,m}}$ and $z = h_{\mathrm{D,M}}$ planes excluding an spherical cap or spherical segment of radius r_{D_0}. Noting that $r_{\mathrm{B_x}} = \sqrt{u_{\mathrm{B_x}}^2 + h_{\mathrm{B}}^2}$, $G_{\mathrm{B_x}} = G_{\mathrm{B}}\left(\pi - \theta_{\mathrm{B_x}}, \theta_{\mathrm{B}}\right)$, and $G_{\mathrm{D_x}} = G_{\mathrm{D}}^{\mathrm{AC}}\left(\pi - \theta_{\mathrm{D_x}}\right)$, where $\theta_{\mathrm{B_x}} = \tan^{-1}(\frac{u_{\mathrm{B_x}}}{h_{\mathrm{B}}})$ and $\theta_{\mathrm{D_x}}$ are the zenith angles of the BS and UAV located at $\mathrm{B_x}$ and $\mathrm{D_x}$, respectively, we obtain the conditional Laplace transform of I as given in the theorem statement. Using this and taking the expectations in (11) over the joint distribution of Z, r_{B_0}, θ_{D_0}, r_{D_0}, and $\phi_{\mathrm{B}_0\mathrm{D}_0}$, we obtain the final result as in (10). ■

REFERENCES

[1] M. Banagar and H. S. Dhillon, "3D two-hop cellular networks with wireless backhauled UAVs: Modeling and fundamentals," *arXiv preprint*, [Online]. Available: https://arxiv.org/abs/2105.07055.

[2] M. Mozaffari *et al.*, "A tutorial on UAVs for wireless networks: Applications, challenges, and open problems," *IEEE Commun. Surveys Tuts.*, vol. 21, no. 3, pp. 2334–2360, 3rd Quart. 2019.

[3] M. Haenggi, *Stochastic Geometry for Wireless Networks*. Cambridge, U.K.: Cambridge University Press, 2012.

[4] H. S. Dhillon, R. K. Ganti, F. Baccelli, and J. G. Andrews, "Modeling and analysis of K-tier downlink heterogeneous cellular networks," *IEEE J. Sel. Areas Commun.*, vol. 30, no. 3, pp. 550–560, Apr. 2012.

[5] H. S. Dhillon and V. V. Chetlur, *Poisson Line Cox Process: Foundations and Applications to Vehicular Networks*. Vermont, USA: Morgan & Claypool Publishers, June 2020.

[6] V. V. Chetlur and H. S. Dhillon, "Downlink coverage analysis for a finite 3-D wireless network of unmanned aerial vehicles," *IEEE Trans. Commun.*, vol. 65, no. 10, pp. 4543–4558, Oct. 2017.

[7] X. Wang *et al.*, "Modeling and analysis of aerial base station-assisted cellular networks in finite areas under LoS and NLoS propagation," *IEEE Trans. Wireless Commun.*, vol. 17, no. 10, pp. 6985–7000, Oct. 2018.

[8] M. Alzenad and H. Yanikomeroglu, "Coverage and rate analysis for vertical heterogeneous networks (VHetNets)," *IEEE Trans. Wireless Commun.*, vol. 18, no. 12, pp. 5643–5657, Dec. 2019.

[9] N. Cherif *et al.*, "Downlink coverage and rate analysis of an aerial user in vertical heterogeneous networks (VHetNets)," *IEEE Trans. Wireless Commun.*, vol. 20, no. 3, pp. 1501–1516, Mar. 2021.

[10] M. Banagar and H. S. Dhillon, "3GPP-inspired stochastic geometry-based mobility model for a drone cellular network," in *Proc. IEEE Global Commun. Conf. (Globecom)*, Dec. 2019.

[11] ——, "Performance characterization of canonical mobility models in drone cellular networks," *IEEE Trans. Wireless Commun.*, vol. 19, no. 7, pp. 4994–5009, July 2020.

[12] M. Banagar, V. V. Chetlur, and H. S. Dhillon, "Handover probability in drone cellular networks," *IEEE Wireless Commun. Lett.*, vol. 9, no. 7, pp. 933–937, July 2020.

[13] W. Lu and M. Di Renzo, "Stochastic geometry modeling and system-level analysis & optimization of relay-aided downlink cellular networks," *IEEE Trans. Commun.*, vol. 63, no. 11, pp. 4063–4085, Nov. 2015.

[14] H. S. Dhillon and G. Caire, "Wireless backhaul networks: Capacity bound, scalability analysis and design guidelines," *IEEE Trans. Wireless Commun.*, vol. 14, no. 11, pp. 6043–6056, Nov. 2015.

[15] N. Kouzayha *et al.*, "Stochastic geometry analysis of hybrid aerial terrestrial networks with mmWave backhauling," in *Proc. IEEE Int. Conf. Commun. (ICC)*, June 2020, pp. 1–7.

[16] M. Gapeyenko *et al.*, "Flexible and reliable UAV-assisted backhaul operation in 5G mmWave cellular networks," *IEEE J. Sel. Areas Commun.*, vol. 36, no. 11, pp. 2486–2496, Nov. 2018.

[17] B. Galkin, J. Kibilda, and L. A. DaSilva, "Backhaul for low-altitude UAVs in urban environments," in *Proc. IEEE Int. Conf. Commun. (ICC)*, May 2018, pp. 1–6.

[18] 3GPP, "Study on 3D channel model for LTE," 3rd Generation Partnership Project (3GPP), Tech. Rep. 36.873, 12 2017.

[19] J. Cho and Z. J. Haas, "On the throughput enhancement of the downstream channel in cellular radio networks through multihop relaying," *IEEE J. Sel. Areas Commun.*, vol. 22, no. 7, pp. 1206–1219, Sep. 2004.

[20] W. L. Stutzman and G. A. Thiele, *Antenna Theory and Design*. John Wiley & Sons, Inc., May 2012.

[21] H. W. Gould, *Combinatorial Identities: Table I: Intermediate Techniques for Summing Finite Series*, May 2010, vol. 4.